Title	Application of Engineered Cementitious Composites to Precast Beam-Column Sub-Assemblage under Column Removal Scenarios
Author(s)	Kang, Shao-Bo; Tan, Kang Hai; Yang, En-Hua
Citation	Kang, S. B., Tan, K. H., & Yang, E. H. (2015) Application of engineered cementitious composites to precast beam-column sub-assemblage under column removal scenarios. fib symposium 2015, Copenhagen, Denmark, 18-20 May.
Date	2015
URL	http://hdl.handle.net/10220/40561
Rights	© 2015 FIP Symposia. This is the author created version of a work that has been peer reviewed and accepted for publication by Symposium 2015, FIP Symposia. It incorporates referee's comments but changes resulting from the publishing process, such as copyediting, structural formatting, may not be reflected in this document. The published version is available at: [http://www.fib-international.org/rss-feed/2015-fib-symposium-copenhagen-registration].

APPLICATION OF ENGINEERED CEMENTITIOUS COMPOSITES TO PRECAST BEAM-COLUMN SUB-ASSEMBLAGE UNDER COLUMN REMOVAL SCENARIOS

Shao-Bo Kang, Kang Hai Tan, En-Hua Yang

School of Civil & Environmental Engineering, Nanyang Technological University, 50 Nanyang Avenue, Singapore 639798

Abstract

This paper presents an experimental study on the behaviour of precast beam-column sub-assemblages under middle column removal scenarios. By using Engineered Cementitious Composites (ECC) in the beam-column joint and the cast-in-situ structural topping, the resistance and deformation capacity of the sub-assemblage was investigated. Besides, the compatible deformation between ECC and longitudinal steel reinforcement was observed at the initial stage, until the tensile strain capacity of ECC was exhausted. With increasing vertical displacement, a major crack was formed in the plastic hinge region, and severe localisation of rotation was recorded at large deformations. Top reinforcement in the beam eventually ruptured near the face of the end column stub, leading to collapse of the sub-assemblage. Conclusion was drawn from the experimental results that application of ECC to the precast beam-column sub-assemblage limits its deformation capacity as a result of higher bond strength between ECC and reinforcing bars.

Keyword: Beam-Column Sub-Assemblage, Catenary Action, Compressive Arch Action, Engineered Cementitious Composites, Progressive Collapse

1 Introduction

Progressive collapse of building structures, such as the Alfred Murrah Federal Building in Oklahoma City and the World Trade Centre in New York, has stirred up extensive research studies on the behaviour of beam-column joints subject to accidental loading conditions. Correspondingly, design approaches have been proposed and incorporated in the design guidelines (DOD 2013; GSA 2003). Among the design approaches, alternate path method is a quantitative method which allows local failure to occur, but seeks to prevent its disproportional propagation through the mobilisation of alternative load path in the bridging beam and the floor system.

Experimental tests on beam-column sub-assemblages and frames indicate that the bridging beam is able to develop compressive arch action and subsequent catenary action when subject to middle column removal scenarios (Sadek & al. 2011; Su, Tian & Song 2009; Yu & Tan 2013). However, development of compressive arch action and catenary action in the beam imposes a high demand on the ductility and integrity of structural joints, in particular for precast concrete structures with weak joints. Therefore, experimental tests are necessary to investigate the behaviour of precast concrete structures under middle column removal scenarios.

Welded connections in precast concrete structures exhibit limited deformation capacity under progressive collapse scenarios (Main & al. 2014). Nevertheless, through proper reinforcement detailing in the joint, precast beam-column sub-assemblages are also capable of developing significant catenary action under column removal scenarios. Besides, innovative cementitious materials can also be used in precast concrete structures to enhance the resistance and deformation capacity. As a high-performance fibre-reinforced concrete, ECC features its strain-hardening behaviour and ultra-high strain capacity in

tension. Therefore, its tensile strength can be considered in design practice (JSCE 2008). It also provides improved bond strength between reinforcement and ECC, thereby reducing the required embedment length in the beam-column joint and reliving congestion of reinforcement (Li 2003). However, its performance under progressive collapse scenarios has not been investigated yet.

The primary objectives of the experimental tests are to evaluate the resistance and rotational capacity of precast ECC beam-column joints subject to progressive collapse scenarios. Besides, the effectiveness of ductile ECC in enhancing the integrity and robustness of precast structures was investigated and conclusions were made based on the experimental results.

2 Experimental programme

A precast concrete structure was designed against gravity loading in accordance with Eurocode 2 (BSI 2004). In order to study the behaviour of precast joints under column removal scenarios, a beam-column sub-assemblage, comprising one 250 mm square middle column stub, one 150 mm by 300 mm double-span beam, was extracted from the precast concrete structure. Two enlarged end column stubs were erected at the ends of the beam, so that horizontal and vertical restraints could be applied on the sub-assemblage.

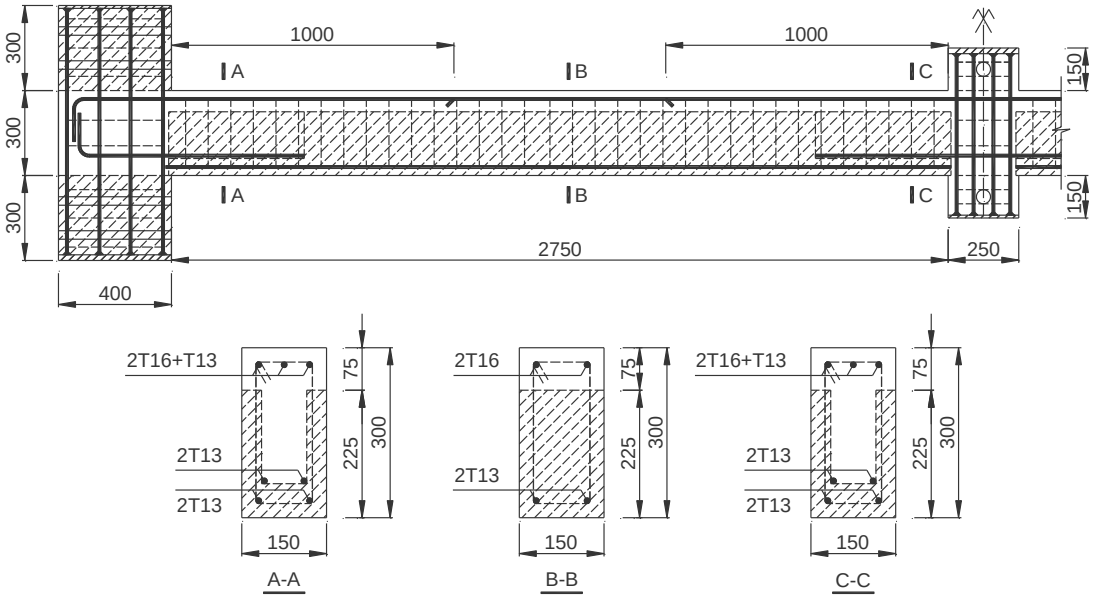

Fig. 1 Geometry and reinforcement detailing of beam-column sub-assemblage

Fig. 1 shows the geometry and the reinforcement detailing of the sub-assemblage. In the precast beam-column sub-assemblage, precast concrete beam units, with troughed section at each end, were prefabricated prior to the cast-in-situ structural topping and the joint. Closely-spaced stirrups were provided along the beam length to ensure the horizontal shear transfer between the precast beam units and the topping. Besides, the horizontal interface was also intentionally roughed to around 3 mm roughness conforming to Eurocode 2 (BSI 2004). The two precast beam units were assembled through short bottom bars placed in the trough and passing through the middle joint. Besides, continuous top longitudinal reinforcement was placed in the beam. Then, the structural topping and joint were cast by using ECC to form the integral sub-assemblage, as shown in Fig. 1. It is notable that the hatched zones in the beam-column sub-assemblage represent the precast beam units.

The test set-up for beam-column sub-assemblages is illustrated in Fig. 2. A point load was applied vertically on the middle joint through a servo-hydraulic actuator, while two horizontal

restraints and one vertical restraint were imposed on each column stub to prevent the horizontal and vertical translations. In addition, two sets of universal columns were erected to prevent the out-of-plane deflection of the beam. In the middle joint, another two groups of short columns and two steel rods were employed to avoid the rotation of the middle beam-column joint after rupture of bottom reinforcement on one side of the joint.

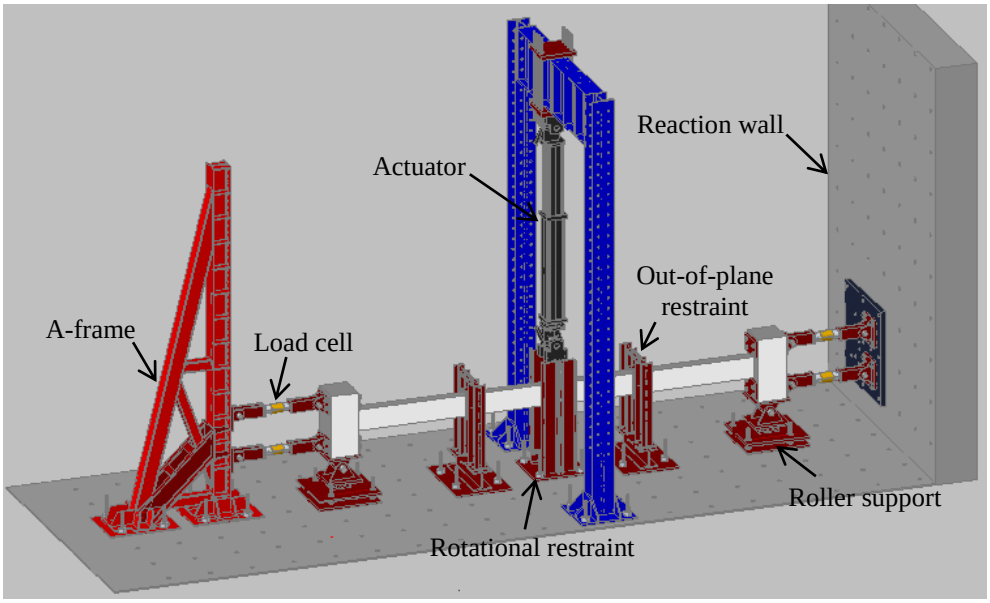

Fig. 2 Test set-up for beam-column sub-assemblage

Due to the limited stiffness of the horizontal restraint, the boundary condition was not ideally rigid, and it weakened the compressive arch action and catenary action behaviour of the beam-column sub-assemblage (Yu 2012). Besides, there might be some connection gaps between the specimen and horizontal restraints. Therefore, a series of linear variable differential transducers (LVDTs), as illustrated in Fig. 3, were used at the two column stubs to monitor the movement of supports and to determine the stiffness of the horizontal restraints and the connection gaps. Additionally, a group of four LVDTs was utilised at each end of the beam to quantify the rotation angle of the plastic hinges, and LVDTs were also placed beneath the beam to measure the vertical displacements at several points. Besides, steel strain gauges were mounted on the longitudinal reinforcing bars. Fig. 4 shows the layout of strain gauges along the beam length. It is notable that only the tensile strains of the longitudinal reinforcement was measured, with the left half representing the top bars at the end column stub and the right half standing for the bottom bars at the middle joint.

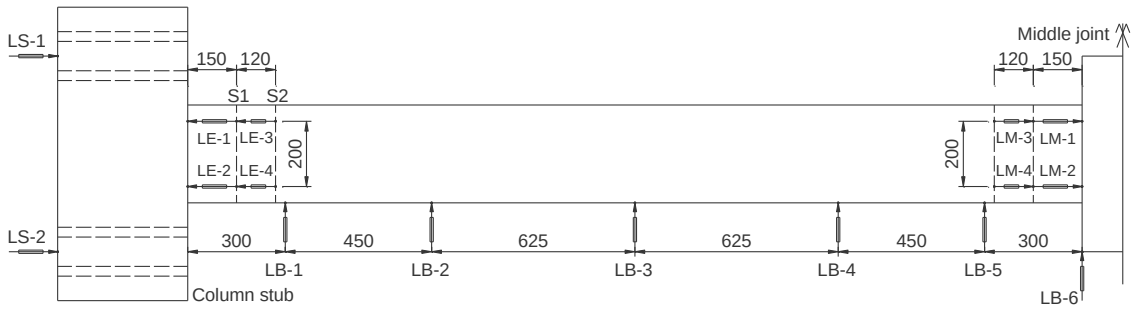

Fig. 3 Layout of LVDTs on sub-assemblage

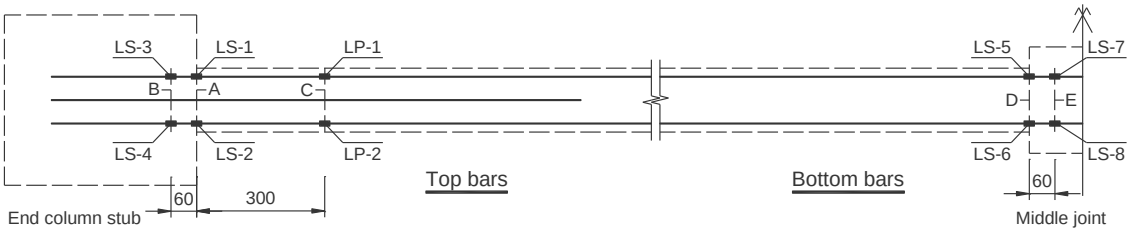

Fig. 4 Layout of strain gauges on the longitudinal reinforcement of the beam

3 Material properties

Prior to testing, material tests were conducted on steel reinforcement and concrete to obtain their respective tensile and compressive strengths. Hot-rolled deformed bars T13 and T16, with yield strengths of 549 MPa and 573 MPa, were used for beam longitudinal reinforcement. The compressive strength of 150 mm diameter by 300 mm high concrete cylinders was determined as 40.5 MPa. Fig. 5 shows the stress-strain curve of one cylinder. The strain represents the average value in a length of 100 mm in the middle of the cylinder. Polyvinyl alcohol fibres with a diameter of 0.044 mm and a length of 12 mm were used in ECC. 50 mm square cubes were tested in compression, and the compressive strength was 62.7 MPa. Besides, the strain-hardening behaviour of ECC was also demonstrated through four-point bending tests of 12 mm thick by 120 mm wide by 300 mm long ECC plates. The clear span of the plate was 240 mm. Fig. 6 shows the load-deflection curve of one ECC plate. It can be observed that after the first cracking the applied load could still increase with increasing deflections until the strain capacity of ECC was reached. The ultimate tensile strain capacity of ECC was calculated as 2.4% through inverse analysis (Qian & Li 2007).

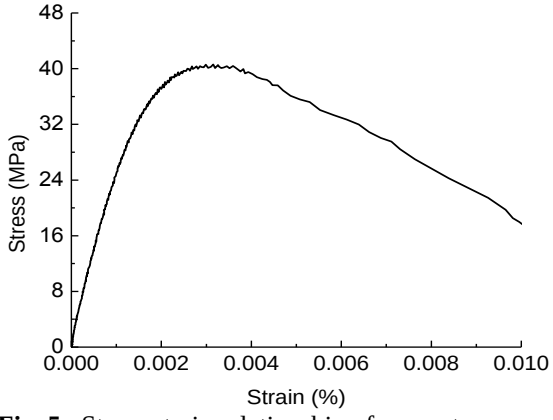

Fig. 5 Stress-strain relationship of concrete

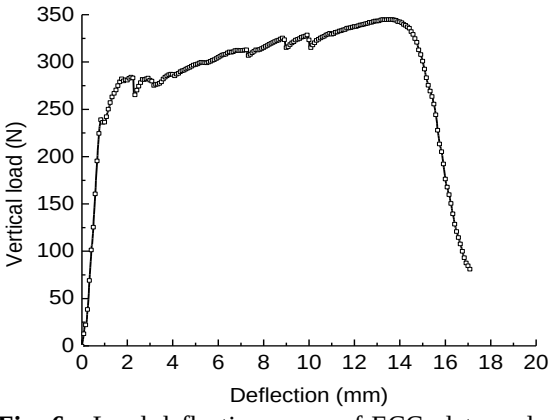

Fig. 6 Load-deflection curve of ECC plate under four-point bending

4 Resistance of beam-column sub-assemblage

Variations of vertical load and horizontal reaction force with middle joint displacement were obtained in the experimental test. Compressive arch action and catenary action sequentially developed in the bridging beam. When the middle joint displacement was less than one beam depth 300 mm, horizontal compression force was generated in the bridging beam and the sub-assemblage was able to develop significant compressive arch action, as shown in Figs. 7 and 8. The maximum compression force in the beam was 305.8 kN, and the compressive arch action capacity of the sub-assemblages was 91.1 kN. Compared with its flexural action capacity of 76.2 kN, the resistance of the sub-assemblage was enhanced by around 20% by the compressive arch action. After the

compressive arch action capacity was achieved, crushing of concrete occurred in the compression zones of the beam, and both the vertical load and the horizontal compression force started to decrease. In the descending branch of the vertical load, rupture of bottom reinforcement at the middle joint interface suddenly reduced the vertical load, but it had minor effect on the horizontal compression force. Following rupture of bottom reinforcement at the left face of the joint, rotational restraint in the middle joint enabled development of sagging moment at the right joint face. Thus, the vertical load increased prior to the commencement of catenary action in the beam.

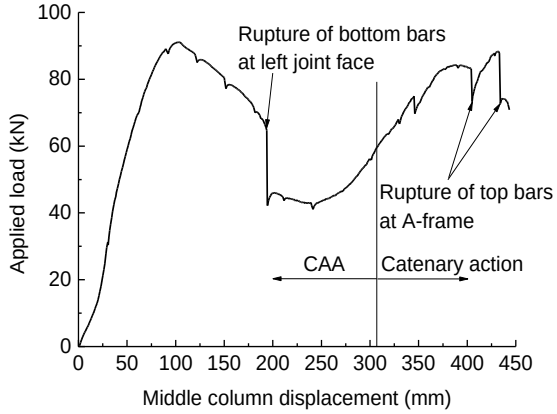

Fig. 7 Vertical load-middle joint displacement curve

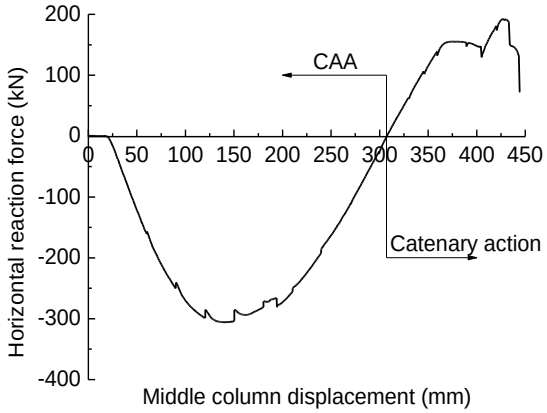

Fig. 8 Horizontal reaction force-middle joint displacement curve

When the vertical displacement of the middle joint surpassed one bean depth, the load continued to increase due to onset of catenary action in the beam, as shown in Fig. 7. At the catenary action stage, horizontal tension force was mobilised in the beam and eventually attained its maximum value of 192.2 kN (see Fig. 8). The sub-assemblage developed the catenary action capacity of 88.3 kN prior to fracture of all the beam top reinforcement at the left end column stub. However, the catenary action capacity was 4% lower in comparison with the compressive arch action capacity. Therefore, it is not effective to act as the last line of defence against progressive collapse if the compressive arch action capacity is exceeded.

5 Deformation capacity of the sub-assemblage

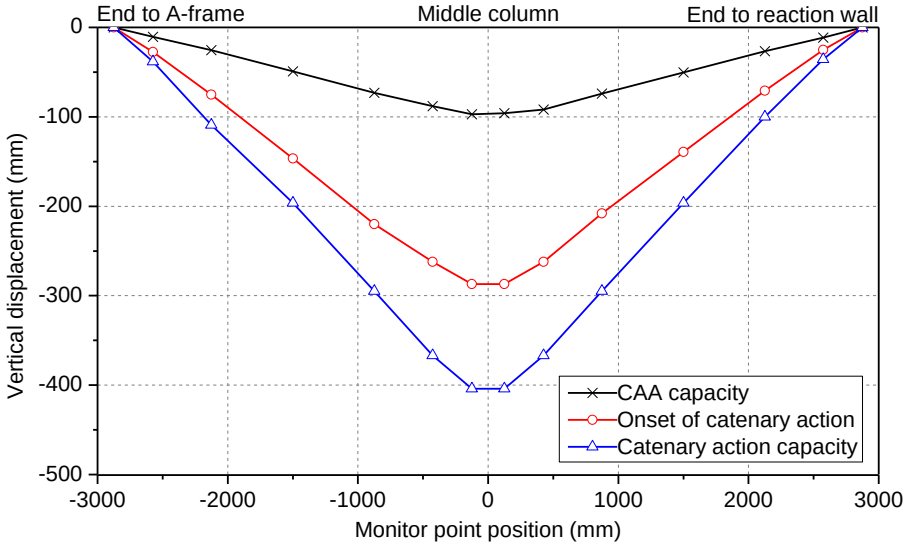

Fig. 9 Deformed profile of the sub-assemblage

Fig. 9 shows the vertical deflections of the sub-assemblages at various loading stages. Different from reinforced concrete beam-column sub-assemblages (Yu & Tan 2013), the single-span beam between the middle joint and the end column stub remained almost rigid, and rotation of the sub-assemblage was concentrated at the beam ends. Thus, the deformation capacity of the sub-assemblage depended on the rotational capacity of plastic hinges at the end column stub, and flexural deformation of the beam contributed little to the total deformation of the sub-assemblage. Therefore, the rotation of the plastic hinges has to be quantified to evaluate the deformation capacity of the sub-assemblage.

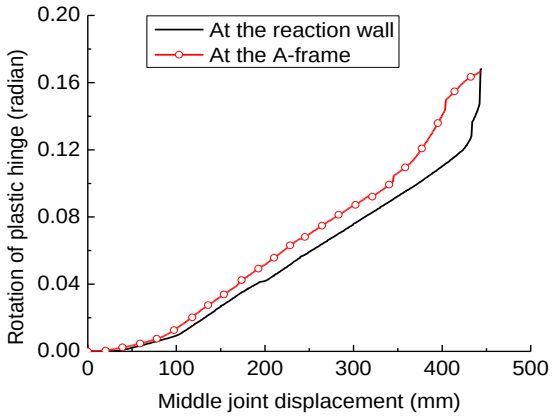

Fig. 10 Rotation angle of plastic hinges at the end column stubs

The rotation of the plastic hinges at the end column stub was measured through four LVDTs in a length of 270 mm. Fig. 10 shows the variation of plastic hinge rotation with middle joint displacement. When the middle joint displacement was smaller than 100 mm, connection gaps between the horizontal restraint and the end column stub allowed free rotation of the stub, and thus the rotation of the plastic hinges increased slowly. After the connection gaps were closed, the plastic hinge rotation increased linearly with middle joint displacement, and no plateau stage was observed, as shown in Fig. 10. When the sub-assemblage attained its catenary action capacity, the plastic hinge ratio at the A-frame was 0.163 radian. Besides, the rotation angle of the sub-assemblage was 0.156 radian, calculated as the middle joint displacement at the catenary action capacity divided by the clear span of the beam.

6 Crack pattern and failure mode of the beam

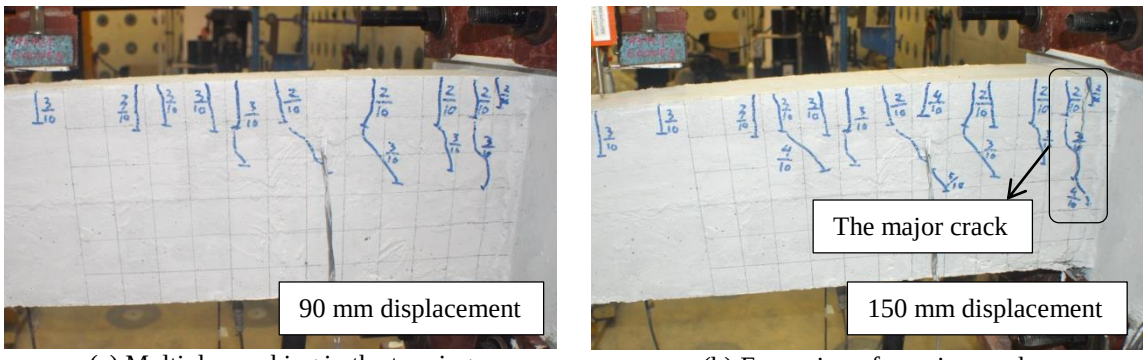

(a) Multiple-cracking in the topping (b) Formation of a major crack

Fig. 11 Development of multiple cracking in the structural topping

In the experimental test, different behaviour of ECC topping was observed with increasing middle joint displacement. At the initial stage, multiple cracks were formed on the topping due to its strain-hardening behaviour and superior strain capacity in tension, as shown in Fig. 11(a). At 120 mm

vertical displacement, a major crack was initiated near the end column stub, as shown in Fig. 11(b), indicating that the tensile strain capacity of ECC was exhausted. The major crack started to propagate towards the compression zone with increasing middle joint displacement. However, away from the major crack, ECC topping was able to sustain tensile stress and the width of the hairline cracks remained at around 0.1 mm.

In the descending branch of the vertical load, bottom reinforcement at the middle joint interface fractured, as shown in Fig. 12(a). However, much less crushing and spalling of concrete was observed in the compression zone at the middle joint due to the improved ductility of ECC in comparison with conventional concrete. Near the end column stub, the major crack was widened with increasing middle joint displacement, as shown in Fig. 12(b). Besides, severe crushing of concrete occurred in the compression zone. At the catenary action stage, axial tension force generated full-depth tension cracks along the beam length (see Fig. 12(c)). However, the spacing of the full-depth cracks on the precast beam units was much larger than that of multiple cracks on the ECC topping. Eventually, localisation of cracks led to premature fracture of beam top reinforcement at the left end column stub, as shown in Fig. 12(c).

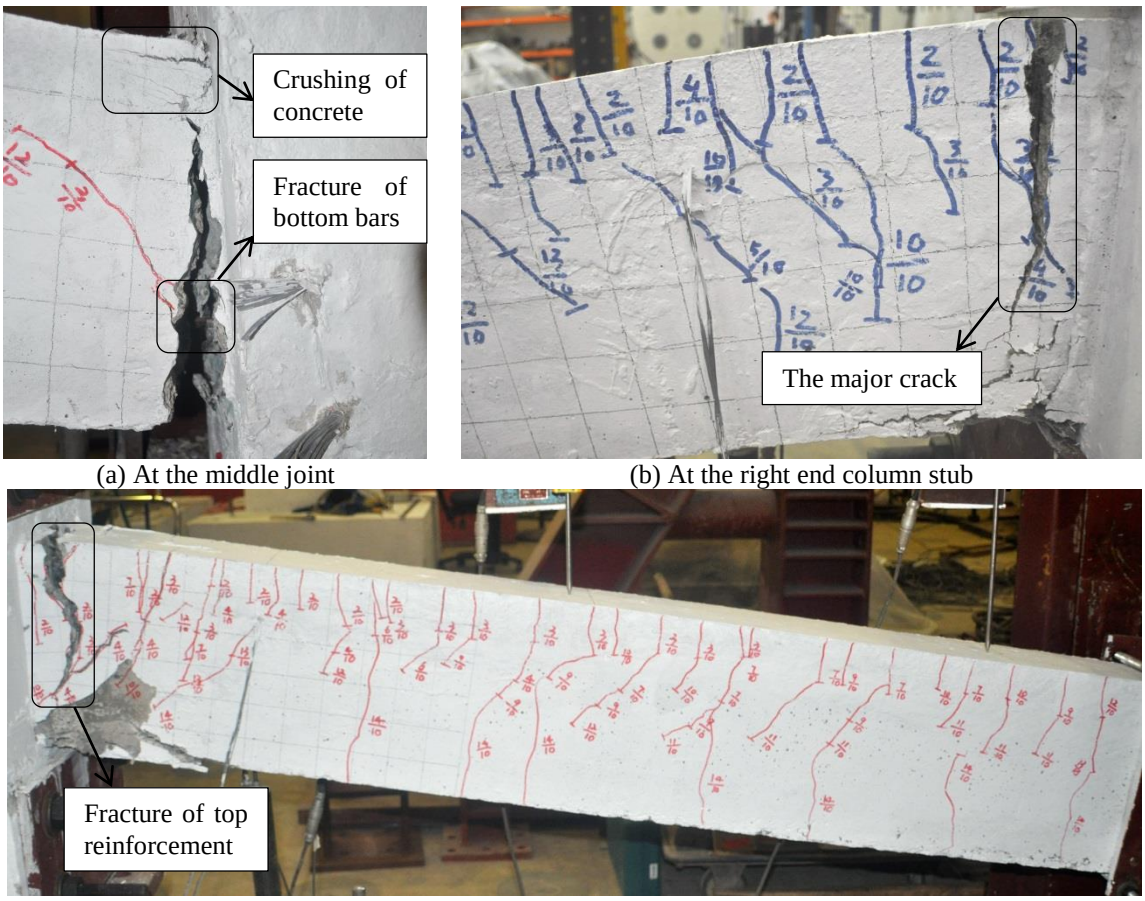

(a) At the middle joint

(b) At the right end column stub

(c) At the left end column stub

Fig. 12 Failure modes of the beam-column sub-assemblage

7 Variation of steel strains

Fig. 13 shows the variation of strains of longitudinal reinforcement at the selected sections. Due to presence of the vertical concrete/ECC interface at the middle joint interface, LS-5 and LS-6 attained their yield strain at 35 mm middle joint displacement, and rapidly developed into the post-yielding stage, as shown in Fig. 13(a). In the middle joint, strains LS-7 and LS-8 were smaller than LS-5 and LS-6 and exhibited a plateau stage as a result of bond strength between ECC and

reinforcement. Similar variation of steel strains was also observed at the end column stub, as shown in Fig. 13(b). However, strains LS-1 and LS-2 increased slowly before ECC topping attained its tensile strain capacity at 120 mm displacement. Besides the middle joint and the end column stub, stain gauges were also mounted at the section 300 mm from the end column stub face, as shown in Fig. 4. LP-1 and LP-2 did not reach the yield strain of steel reinforcement when rupture of beam top reinforcement occurred at the end column stub. It indicates that with ECC used in the structural topping, the length of plastic hinge was less than one beam depth 300 mm. This behaviour possibly results from higher bond strength between ECC and reinforcement.

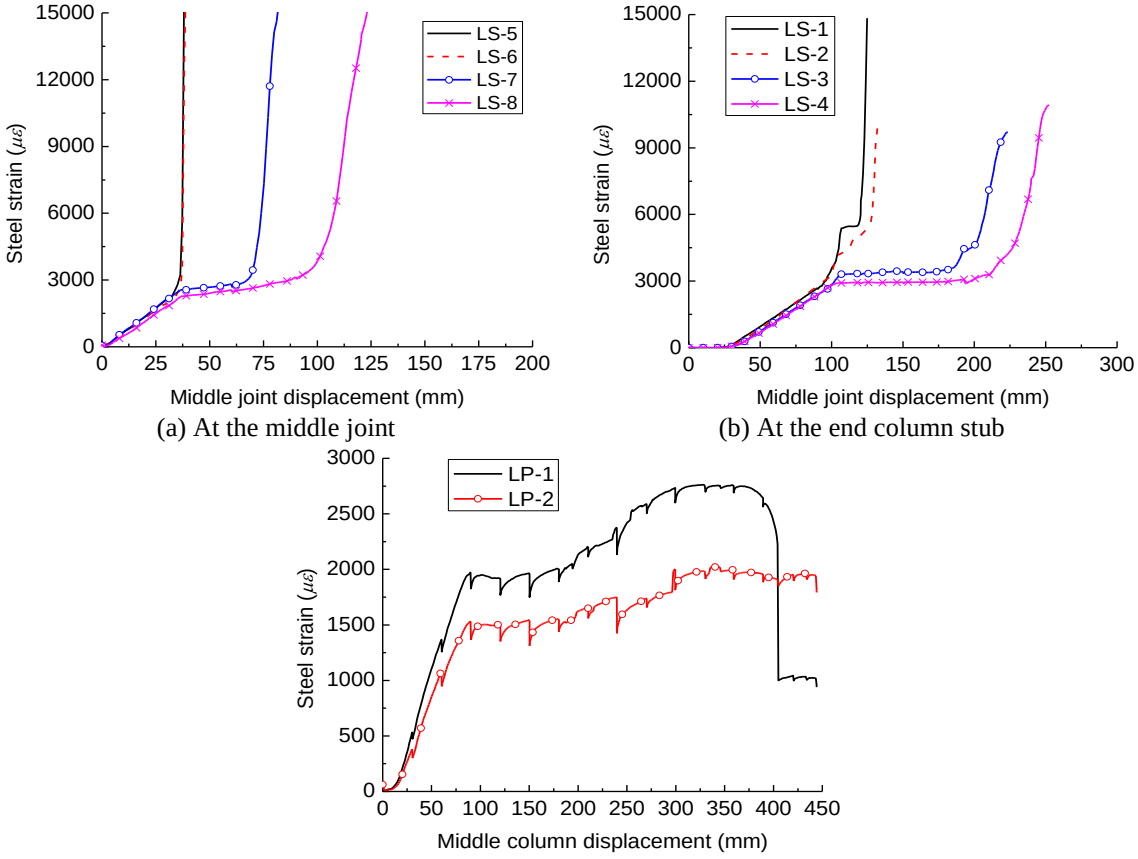

(a) At the middle joint

(b) At the end column stub

(c) At the curtailment point of top bars

Fig. 13 Variation of steel strains with middle joint displacement

8 Conclusions

When ECC with tensile strain-hardening behaviour and ultra-high strain capacity was utilised in the joint and structural topping of precast beam-column sub-assemblages, multiple cracking on the structural topping was observed at relatively small middle joint displacement. Steel reinforcement and ECC sustained tension force compatibly when the compressive arch action capacity of the sub-assemblage was attained. Thus, ECC was effective in enhancing the resistance of the sub-assemblage at the compressive arch action stage. However, a major crack was formed near the end column stub at about 150 mm middle joint displacement. With increasing middle joint displacement, deformation of the beam was concentrated at the major crack, while ECC topping remained at the multi-cracking stage and was effective in resisting tensile stress away from the major crack. The localised crack eventually led to premature fracture of top longitudinal reinforcement in the beam, thereby hindering development of catenary action. Therefore, in design of precast beam-column sub-assemblages against progressive collapse, the tensile strength of ECC

can be considered at the compressive arch action stage. However, its strain-hardening behaviour in tension limits its potential application to large deformation scenarios.

Acknowledgements

The authors acknowledge the support for the research project “Integrated Structures and Materials Design for Precast Concrete 66 kV Substation against Progressive Collapse” provided by JTC Corporation, Singapore.

References

BSI (2004). "Eurocode 2: Design of concrete structures—Part 1-1: General rules and rules for buildings." BS EN 1992-1-1:2004, British Standards Institution, London, 225.

DOD (2013). "Design of Buildings to Resist Progressive Collapse." Unified Facilities Criteria(UFC)-4-023-03, Department of Defence, Washington, DC.

GSA (2003). "Progressive Collapse Analysis and Design Guidelines for New Federal Office Buildings and Major Modernization Projects." General Services Administration, Washington, DC.

JSCE (2008). "Recommendations for Design and Construction of High Performance Fiber Reinforced Cement Composites with Multiple Fine Cracks (HPFRCC)." Concrete Engineering Series 82, Japan Society of Civil Engineers.

Li, V. C. (2003). "On Engineered Cementitous Composites (ECC)-A Review of the Material and Its Applications " Journal of Advanced Concrete Technology, 1(3), 215-230.

Main, J. A., Bao, Y., Lew, H. S., and Sadek, F. (2014). "Robustness of Precast Concrete Frames: Experimental and Computational Studies." Structures Congress 2014, 2210-2220.

Qian, S., and Li, V. C. (2007). "Simplified Inverse Method for Determining the Tensile Strain Capacity of Strain Hardening Cementitious Composites." Journal of Advanced Concrete Technology, 5(2), 235-246.

Sadek, F., Main, J. A., Lew, H. S., and Bao, Y. (2011). "Testing and analysis of steel and concrete beam-column assemblies under a column removal scenario." Journal of Structural Engineering, 137(9), 881-892.

Su, Y., Tian, Y., and Song, X. (2009). "Progressive collapse resistance of axially-restrained frame beams." ACI Structural Journal, 106(5), 600-607.

Yu, J. (2012). "Structural Behaviour of Reinforced Concrete Frames Subjected to Progressive Collapse." PhD thesis, Nanyang Technological University, Singapore.

Yu, J., and Tan, K. H. (2013). "Experimental and Numerical Investigation on Progressive Collapse Resistance of Reinforced Concrete Beam Column Sub-assemblages." Engineering Structures, 55, 90-106.